SMC-TR-97-01

AEROSPACE REPORT NO.
TR-97(1306)-1

K-2 Titan IV Stratospheric Plume Dispersion

10 January 1997

Prepared by

E. J. BEITING
Mechanics and Materials Technology Center
Technology Operations

R. A. KLINGBERG
Space and Environment Technology Center
Technology Operations

Prepared for

SPACE AND MISSILE SYSTEMS CENTER
AIR FORCE MATERIEL COMMAND
2430 E. El Segundo Boulevard
Los Angeles Air Force Base, CA 90245

Space Technology Applications

THE AEROSPACE CORPORATION
El Segundo, California

This report was submitted by The Aerospace Corporation, El Segundo, CA 90245-4691, under Contract No. F04701-93-C-0094 with the Space and Missile Systems Center, 2430 E. El Segundo Blvd., Los Angeles Air Force Base, CA 90245. It was reviewed and approved for The Aerospace Corporation by S. Feuerstein Principal Director, Mechanics and Materials Technology Center. John R. Edwards was the project officer for the program.

This report has been reviewed by the Public Affairs Office (PAS) and is releasable to the National Technical Information Service (NTIS). At NTIS, it will be available to the general public, including foreign nationals.

This technical report has been reviewed and is approved for publication. Publication of this report does not constitute Air Force approval of the report's findings or conclusions. It is published only for the exchange and stimulation of ideas.

John R. Edwards
SMC/CEV

REPORT DOCUMENTATION PAGE

Form Approved
OMB No. 0704-0188

1. AGENCY USE ONLY (*Leave blank*)	2. REPORT DATE	3. REPORT TYPE AND DATES COVERED
	10 January 1997	

4. TITLE AND SUBTITLE
K-2 Titan IV Stratospheric Plume Dispersion

5. FUNDING NUMBERS
F04701-93-C-0094

6. AUTHOR(S)
E. J. Beiting and R. A. Klingberg

7. PERFORMING ORGANIZATION NAME(S) AND ADDRESS(ES)
The Aerospace Corporation
Technology Operations
El Segundo, CA 90245-4691

8. PERFORMING ORGANIZATION REPORT NUMBER
TR-97(1306)-1

9. SPONSORING/MONITORING AGENCY NAME(S) AND ADDRESS(ES)
Space and Missile Systems Center
Air Force Materiel Command
2430 E. El Segundo Boulevard
Los Angeles Air Force Base, CA 90245

10. SPONSORING/MONITORING AGENCY REPORT NUMBER
SMC-TR-97-01

11. SUPPLEMENTARY NOTES

12a. DISTRIBUTION/AVAILABILITY STATEMENT
Approved for public release; distribution unlimited

12b. DISTRIBUTION CODE

13. ABSTRACT (*Maximum 200 words*)

Video images were recorded of the plume from the K-2 Titan IV launched 2 July 1996 from Cape Canaveral Air Station. These images were used to infer plume motion and expansion near an altitude of 30 km in the stratosphere. The plume was observed to move across the sky in a generally east-to-west direction with a speed of 19±2 km/s. The plume diameter at an altitude of 30 km was measured for 12 min and found to increase as a linear function of time with a rate of 0.48±0.03 km/min. The diameter of a bulge that appeared in the plume at an altitude of 29.5 km was measured for 7 min and also was found to increase linearly with a rate of 0.60±0.07 km/min. The angular width of the plume increased to a value greater than the field-of-view of the cameras, restricting the observation times to those listed. The plume was visible at both visible and near-infrared wavelengths with good contrast until sunset at altitude, which occurred 15 min after vehicle passage.

14. SUBJECT TERMS
Solid rocket motor exhaust, Stratospheric plume, Plume expansion, Stratospheric wind

15. NUMBER OF PAGES
22

16. PRICE CODE

17. SECURITY CLASSIFICATION OF REPORT	18. SECURITY CLASSIFICATION OF THIS PAGE	19. SECURITY CLASSIFICATION OF ABSTRACT	20. LIMITATION OF ABSTRACT
UNCLASSIFIED	UNCLASSIFIED	UNCLASSIFIED	

Acknowledgments

This work greatly benefited from the timely cooperation of many individuals within The Aerospace Corporation. Dr. Thomas Knudtson of Environmental Monitoring & Technology Dept. provided excellent managerial support both at AGO and at the Eastern Test Range. Environmental Systems (Mr. Noble Dowling, Dr. Martin Ross, and Dr. Bart Lundbladt) aided in gaining access to the Eastern Test Range during the launch. Mr. Roy Ehlers of the Flight Mechanics Dept. and Mr. Bruce Mau of Titan Mission Assurance gave timely response in providing the K-2 trajectory before the launch and the telemetry data after the launch, respectively. Dr. Robert Abernathy of the Environmental Monitoring & Technology Dept. provided digitized maps and coordinates of a number sites around the launch facility. Mr. Douglas Schulthess at the Eastern Test Range gave excellent support before, during, and after the launch, providing maps, landmark identification, procedures, etc. required for the acquisition and reduction of the data. The efficiency and cooperative spirit of these individuals made this operation successful and economical. This work was sponsored by Environmental Programs under the direction of Dr. Thomas Spiglanin in support of the Environmental Management Branch of SMC (AXFV) led by Mr. John Edwards.

Contents

Figures

Tables

1. Background

Recent chemical models of solid rocket motor (SRM) exhaust predict that stratospheric ozone levels in the plume will be depressed from ambient values by after-burning HCl.[1–6] Although the size and persistence of the predicted reduced ozone concentrations are a sensitive function of the plume dispersion rate, data measuring this rate are nearly nonexistent.[7] The total database for this parameter consists of a single plume expansion rate of an unidentified rocket (presumably a Titan III) measured by photographic cameras placed at three ground positions taken more than 20 years ago. These data measured expansion of the plume at the lower edge of the stratosphere (18 km) for 10 min after vehicle passage and were presented in a committee report.[8] The expansion rate reported was about an order of magnitude greater than that used in some of the models of SRM stratospheric plume chemistry. More recently, a plume expansion rate at an altitude of 30 km (also observed for 10 min after vehicle passage) was made from an existing video tape of a recent STS plume.[7] This rate is about a factor of 2 greater than the rate measured at 18 km. Currently, there are no measurements of plume expansion as a function of altitude, as a function of launch conditions, and for longer than 10 min after vehicle passage.

In order to add to this limited database, a series of ground-based measurements are planned using cameras to image the plume. It appears possible to enhance the contrast of the image of the plume against the bright sky by placing spectral and polarizing filters in front of the lenses of these cameras. This enhancement technique exploits the different polarization characteristics of sunlight that is Rayleigh-scattered from the troposphere and sunlight that is Mie-scattered from the plume in the stratosphere. This contrast enhancement should permit the observation time to be increased beyond the 10 min previously attainable. Measuring plumes for several launches will allow the variation of the plume expansion rate to be studied as a function of stratospheric conditions. Imaging the plume from at least two appropriately placed ground positions will permit the diameters to be measured and permit differentiation between plume expansion and plume shearing. This differentiation is important since expansion dilutes the chemical concentrations in the plume and changes the rate of the chemical reactions, whereas shearing simply segments parcels of the plume without dilution. The instruments for acquiring these images are currently being built. This report presents data from an initial measurement in this sequence that used an existing instrument to measure the plume expansion of a Titan IV vehicle. Although this instrument was not ideal for this application, it did permit the measurements to be made with little lead time in order to take advantage of an nearly ideal launch window.

2. Launch Details

2.1 Viewing Geometry

K-2 was launched from Space Launch Complex 40 (SLC-40) and was viewed from Universal Camera Site 7 (USC-7) of the Kennedy Space Center. These sites are shown in Figure 1; their coordinates, along with other useful sites shown in Figure 1, are given in Table 1. USC-7 is 6.7 km north and 2.9 km west of SLC-40. The view from USC-7 to SLC-40 in shown in Figure 2. Most of the features identified in this photograph are part of SLC-41 and were used to verify the calibration of the field-of-view (FOV) of the cameras.

The approximate vehicle ground track and the ground projection of the observation line-of-site vector at two times is also indicated in Figure 1. There was a considerable change in the azimuth of the cameras as they tracked the vehicles during ascent. This change in azimuth was useful in assuring that the different altitudes were well separated during the plume expansion. In this respect, an observation site with a viewing vector orthogonal to the ground projection of the vehicle track at the desired altitude is the most advantageous. A three-dimensional plot of the viewing vector and the vehicle trajectory is shown in Figure 3. Plots of the predicted vehicle altitude and distance and as a function of time and the predicted azimuth and elevation as a function of altitude are shown in Figure 4. The values in these plots were calculated from geodetic latitude, longitude, and altitude predictions made by a general trajectory simulation, three degree of freedom (GTS 3DOF) algorithm.[9] These values were used for planning the mission. Similar plots made from the telemetry data received after the launch are presented in Figure 5 and show little difference from the predicted values given in Figure 4 on the scale presented.

Table 1. Coordinates of Sites Indicated in Figure 1

Site	Latitude	Longitude
SLC-34	28.520	-80.563
SLC-40	28.562	-80.577
SLC-41	28.5834	-80.5829
UCS-02	28.527	-80.623
UCS-07	28.622	-80.607
UCS-15	28.578	-80.608
ITL	28.518	-80.586
Static Test Road	28.532	-80.616
Press Site	28.584	-80.646
Banana River	28.610	-80.670

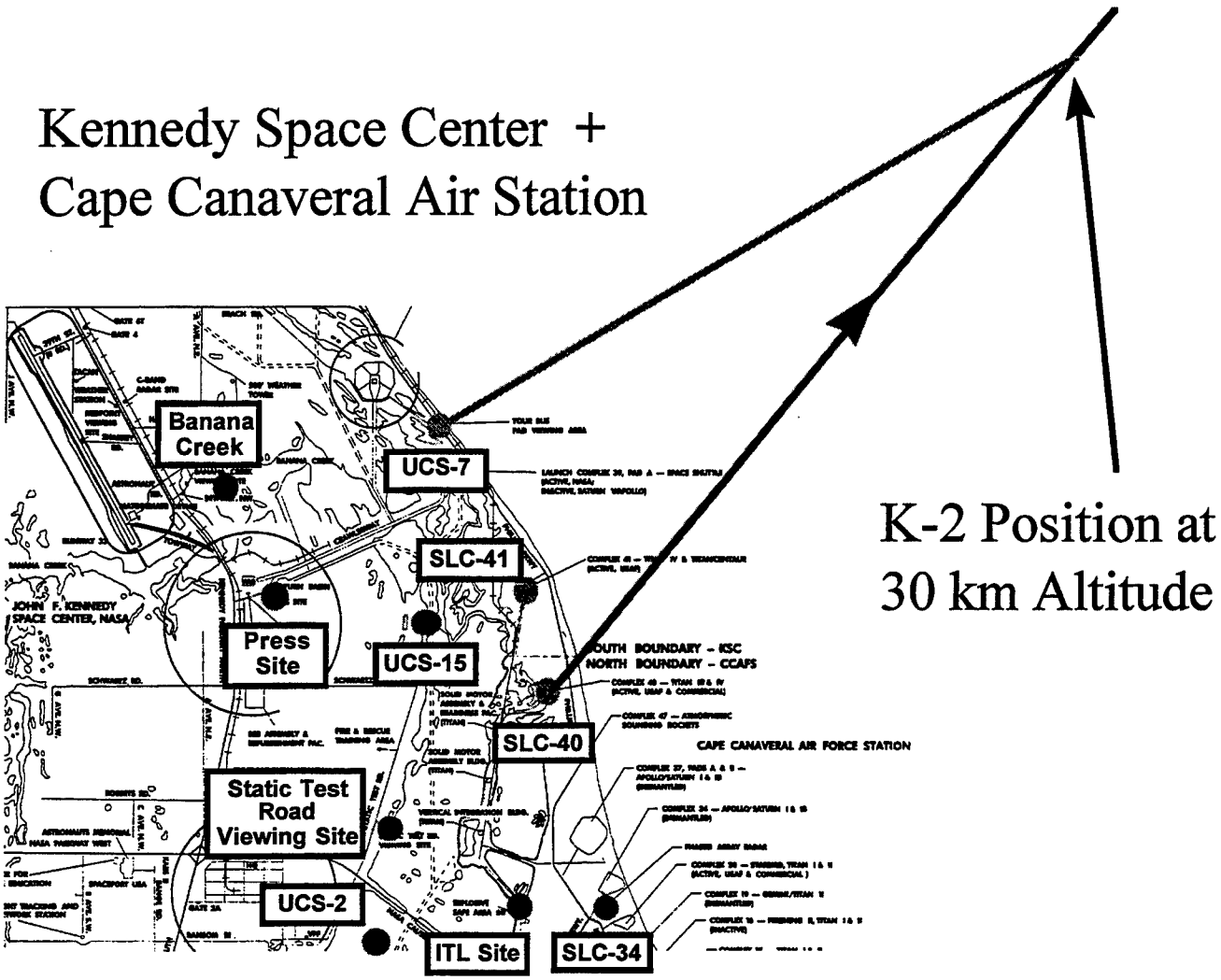

Figure 1. Map showing the launch and observation positions. The vehicle track and ground projection of viewing line are indicated for an altitude of 30 km.

Figure 2. View of the K-2 vehicle before launch from USC-7. The objects identified in the photograph were used to verify the field-of-view measurements made in the laboratory given in Section 3. From left to right, the objects are: (1) SLC-41 NE lightning tower; (2) SLC-41 Mobile Service Tower; (3) Pad 39A J8-1513 LH2 Facility; (4) SLC-41 SW lightning tower; (5) SLC-40 SE lightning tower; (6) SLC-40 Mobile Service Tower; (7) SLC-40 UT and rocket; (8) Pad 39A J8-1611 Flarestack; (9) Pad 39A J8-1610 Water Tank.

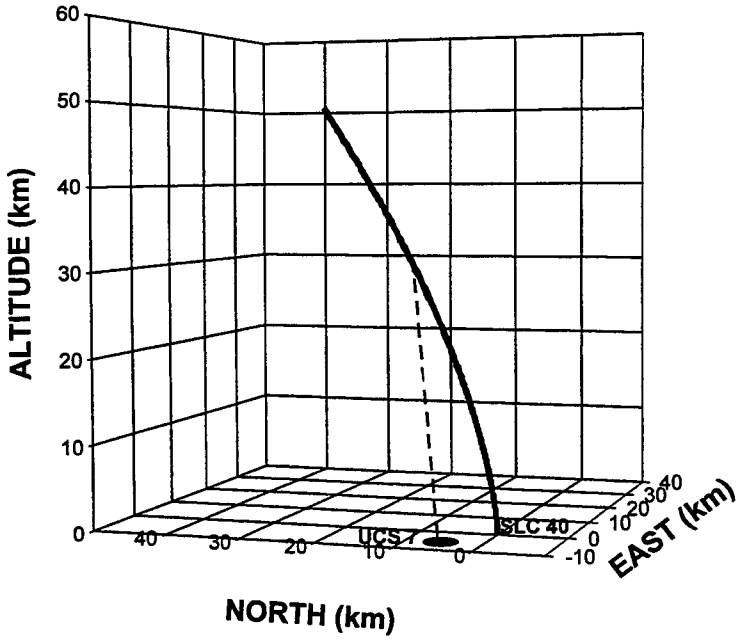

Figure 3. Three-dimensional view of the experimental geometry.

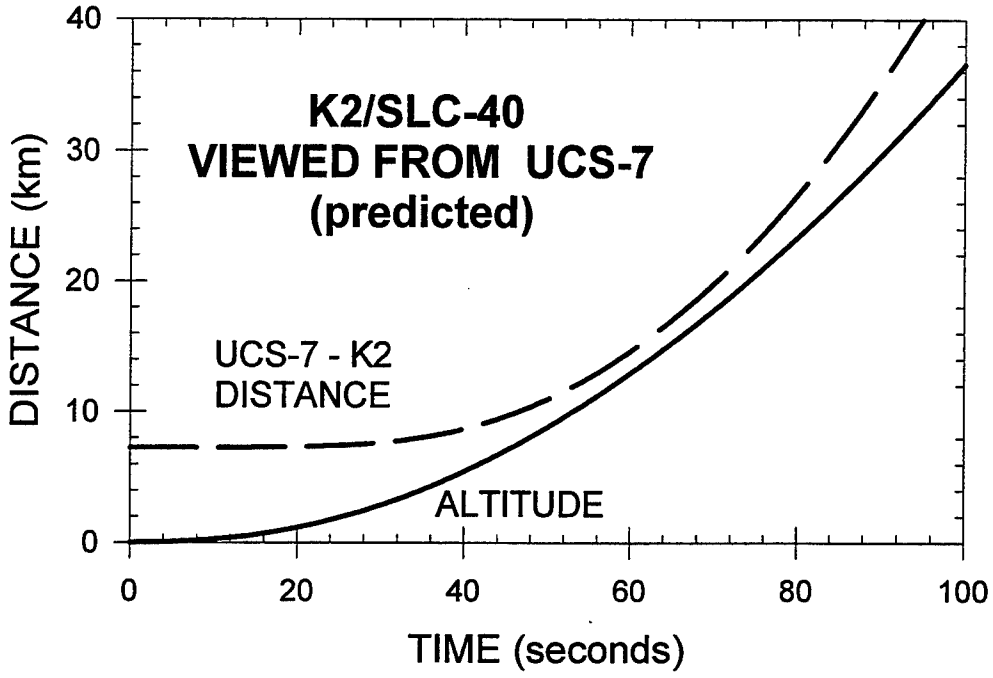

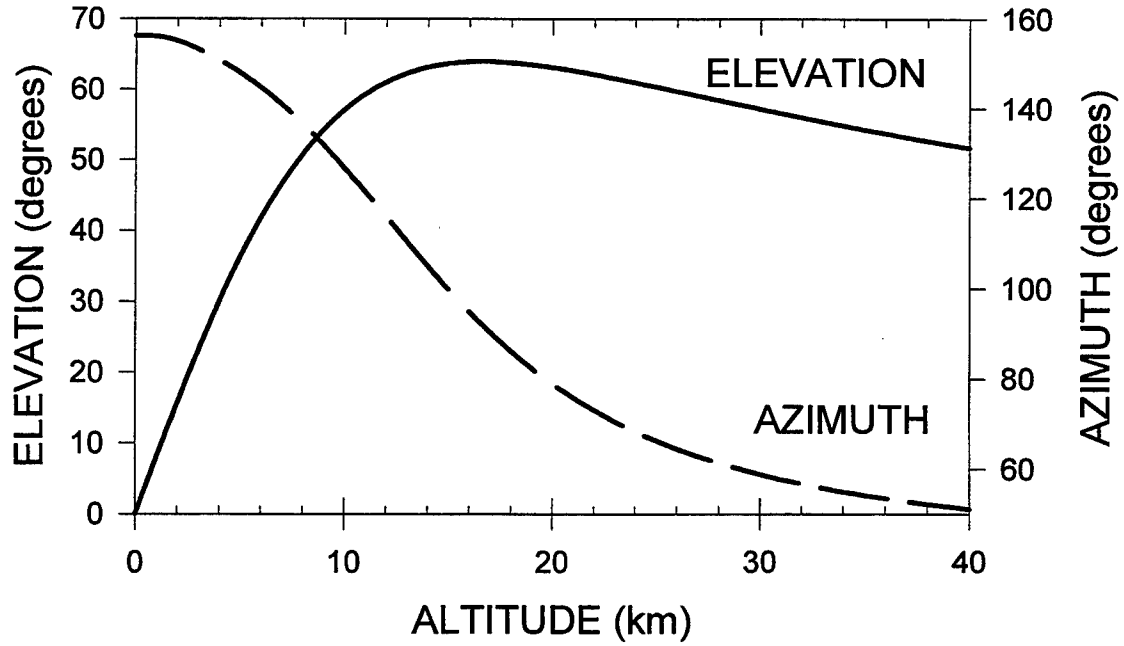

Figure 4. Plots of the predicted vehicle altitude and distance and as a function of time and the predicted azimuth and elevation as a function of altitude calculated from the geodectic latitude, longitude, altitude prediction of Ref. 9.

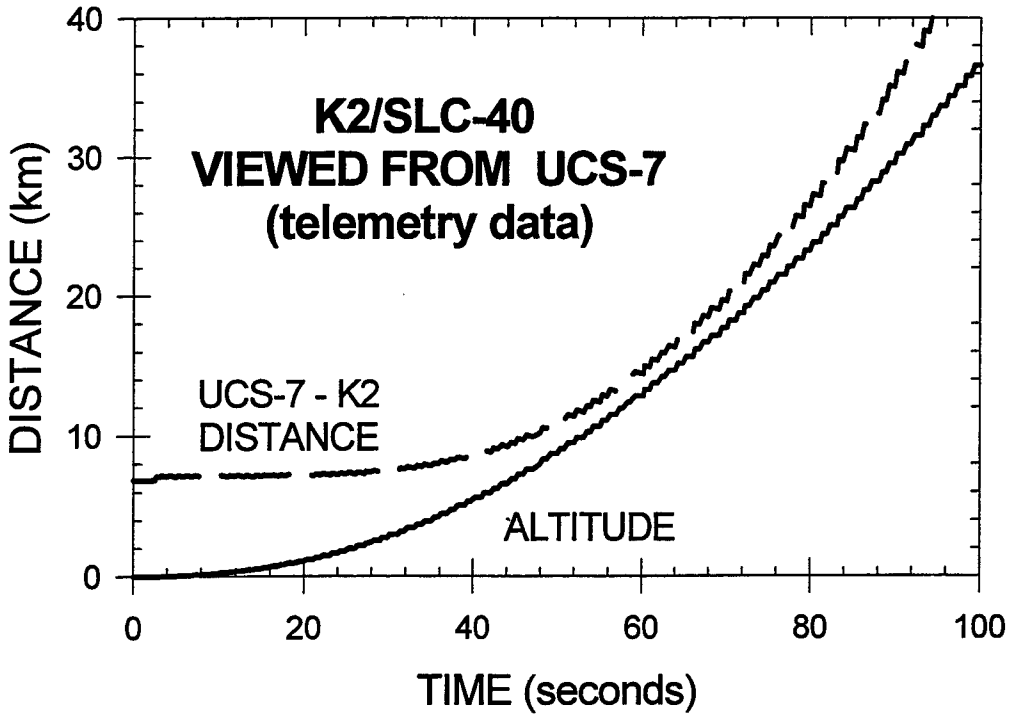

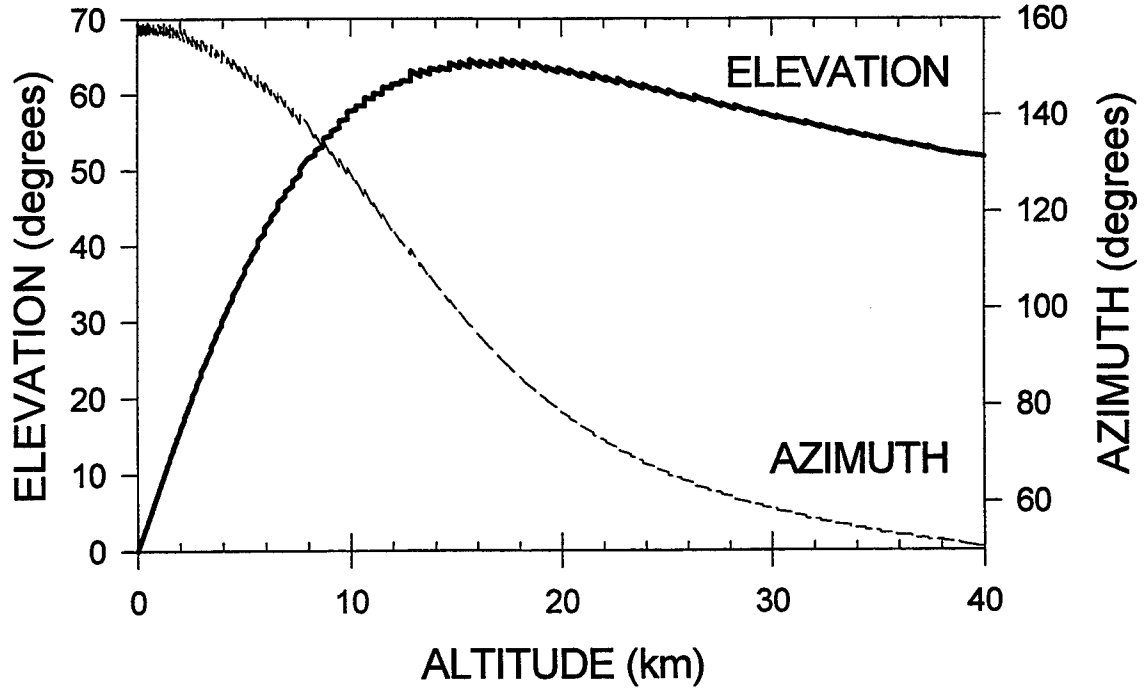

Figure 5. Plots of actual vehicle altitude and distance and as a function of time and the actual azimuth and elevation as a function of altitude calculated from the telemetry data.

2.2 Plume Illumination

K-2 was launched 3 July 1996 at 00:30 GMT (2 July 1996 at 20:30 EDT). Local sunset was 00:24 GMT (20:24 EDT). [10] Thus, the vehicle was launched 6 min after local sunset at ground level. The time between ground-level sunset and sunset at any altitude can be estimated using the expression given Figure 6. The value of 15°/h given for ω is correct for a location on the equator at equinox when the sun travels in a direct east-west arc through the zenith. The variation of ω with date and latitude is complex, but because the launch took place within 1 week of summer solstice when the peak elevation of the sun was about 5° from zenith (latitude of 28.5°–23.5°), this value for ω is approximately correct. The stratospheric altitudes of interest for this work are between 18 and 30 km. Since the instrument afforded only one viewing angle and the launch occurred after ground-level sunset, a viewing angle corresponding to an altitude of 30 km was chosen to permit the greatest viewing time before sunset at altitude. Using this simple formula, sunset was projected to occur 22.2 min after ground-level sunset at 30 km. This agreed with the observation that the plume went dark 15 min after data acquisition began (launch 6 min after ground level sunset + 1.5 min for vehicle to reach 30 km + 15 min observation time = 22.5 min).

The launch time was very close to ideal for this experiment. Because the troposphere (where 95% of the air molecules reside) was unlit, all light scattering came from the SRM plume particles, and this signal did not have to compete with background Rayleigh scattering from the air molecules. Therefore, contrast was excellent, and, for this launch, there was no need for polarization filters to cancel the Rayleigh scattering.

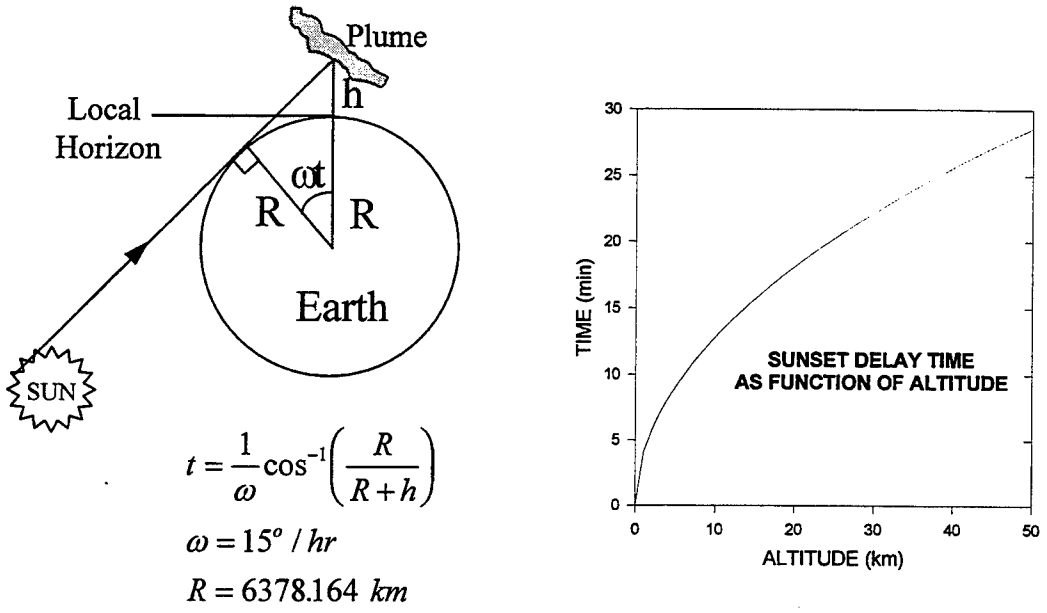

Figure 6. Estimated time interval after ground sunset of sunsets at higher altitudes. The value of 15°/hr is an approximation for the date and latitude of the launch.

3. Instrument

The instrument comprised five video cameras that were fixed to look at a single position in the plume. This system was designed to study the effects of polarization on images of terrestrial objects (particulate laden water, desert soil, boat wakes, etc.).[11] Specifically, the system included five Hatachi KP-140 solid-state CCTV cameras, each connected to a JVC BR-S405U portable video cassette S-VHS recorder as shown in Figure 7. The frames from the cameras could be synchronized, and time signals from a satellite clock receiver[12] were recorded on one audio channel of each recorder. The second set of audio channels was used for voice annotation though a microphone. Four of the cameras were locked in a rigid housing that forced each camera to view the same scene except for the small parallax caused by the stacked vertical mounting (see Figure 8). Each of these four cameras had their internal infrared blocking filter removed and was configured with an external lens, spectral filter, and polarizer. The polarizers were ganged to require the simultaneous rotation through a single knob. The gearing of the polarizer rotation assembly did not permit a rotation rate fast enough to allow the effect of an change in the polarization to be easily discerned by eye. A fifth camera was an unmodified KP-140 mounted adjacent to the bottom of the stack of cameras and aimed to view the same scene. A polarizer mounted on this camera could be adjusted independently from the other four cameras. All five cameras were mounted on a single tripod.

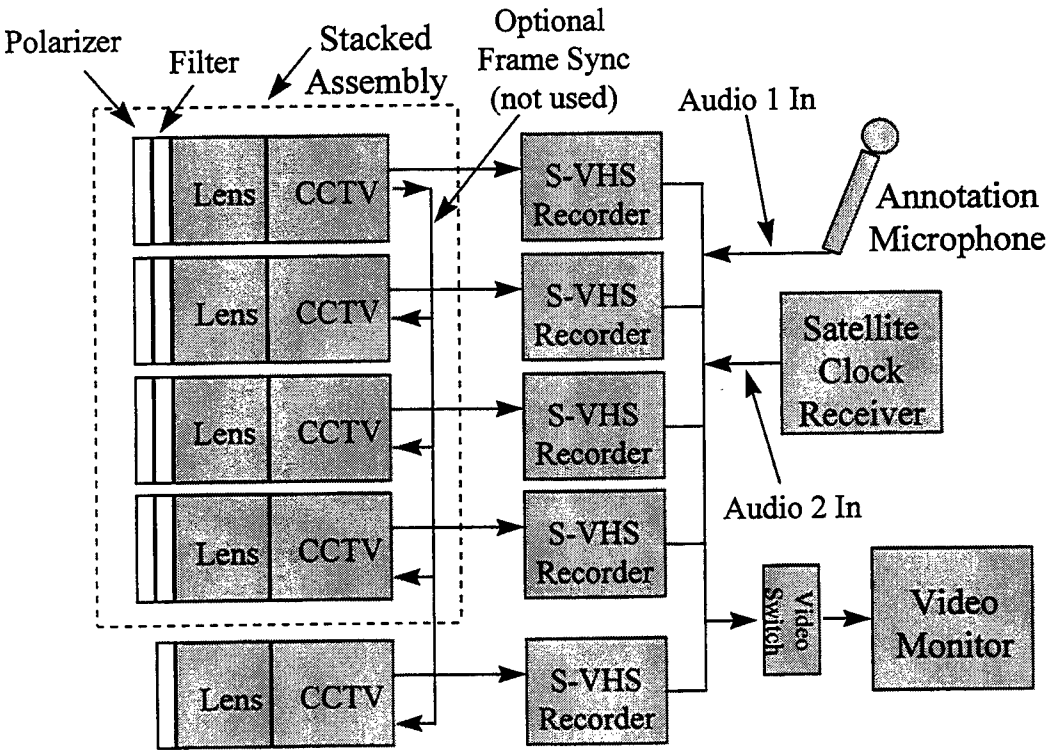

Figure 7. Video components used for recording the K-2 plume expansion. The configuration of each camera is given in Table 2. The output from each camera could be viewed by a video monitor. The GOES satellite clock receiver used an IRIG-B output format.

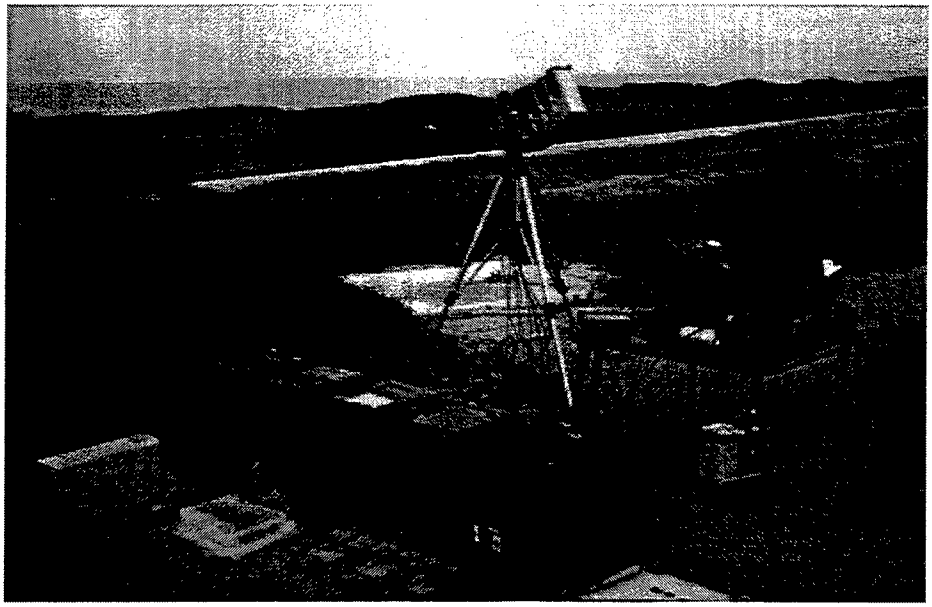

Figure 8. Photograph of the video instrument used to record the K-2 plume expansion. The cameras are directed to approximately the initial elevation and azimuth angles of the SRM plume.

The lenses, filters, polarizers, and FOVs of the cameras are given in Table 2. The FOV values presented in this table were measured using a tripod-mounted encoder with an accuracy of $< \pm 0.03°$ and verified at UCS-7 using the objects identified in Figure 2. Calibrating the FOV of the cameras *in situ* using even very accurately surveyed objects yielded an uncertainty of about $\pm$ 0.5° due to the uncertainty in the exact position of the cameras.

Table 2. Camera Parameters

Camera No.	Lens (mm)	F# Setting	Spectral Filter	Polarizer	FOV (deg)
1	Nikkor 50 mm FL F# 1.2	2.8	510 nm 90 nm FWHM 75% max transmission	Melles Griot 03FPG007 Dichoic Sheet	8.86 H 6.65 V
2	Nikkor AF 24 mm FL F# 2.8	2.8	510 nm 90 nm FWHM 75% max transmission	Melles Griot 03FPG007 Dichoic Sheet	18.51 H 14.04 V
3	Nikkor 50 mm FL F# 1.2	2.0	700-900 nm 40% max transmission	Melles Griot 03FIG005 Near IR	8.78 H 6.59 V
4	Nikkor AF 24 mm FL F# 2.8	2.8	700-900 nm 40% max transmission	Melles Griot 03FIG005 Near IR	18.61 H 14.04 V
5	Nikkor AF 24 mm FL F# 2.8	2.8	Factory Internal	Melles Griot 03FPG007 Dichoic Sheet	not measured

4. Results

4.1 Data Acquisition and Analysis Procedures

The procedure used to acquired the data was straightforward. The cameras were focused on infinity, and the apertures were preset so that clouds in the area viewed at the time of ground-level sunset produced high-contrast images on a video monitor. The aperture settings used during data acquisition are given in Table 2. The angle of the polarizers was preset to view light polarized parallel to the scattering plane (the plane defined by the camera position, the point observed in the plume, and the position of the sun). The cameras imaged SLC-40 during countdown and followed the vehicle during ascent for 90 s. The azimuth and elevation of the cameras then were fixed temporarily so that the vehicle position at T+90 s was near the center of the FOV. This position corresponded to an altitude of 30 km (see Figures 4 and 5). After a few seconds of plume expansion, a bulge appeared near this 30 km position, and this bulge was used to locate the 30 km position at all subsequent times. The azimuth and elevation of the cameras were adjusted as required to keep this feature in view as the plume blew across the sky.

Data analysis was equally straightforward. The video tapes were played on a S-VHS player and viewed on a large monitor (horizontal dimension = 41.3 cm; vertical dimension = 30.6 cm). At time T = +90 s, a timer was started and used to record the expansion time. Measurements of the linear widths perpendicular to the direction of the vehicle track were taken directly from the screen with an estimated accuracy of ± 10% and then converted to angular widths using FOV values given in Table 2. These angular widths were converted to plume widths by noting that

$$w = 2D(t)\sin(\Delta\alpha/2), \tag{1}$$

where w is the width of the plume, $D(t)$ is the distance from the camera to the plume, and $\Delta\alpha$ is the angular width. Note that $D(t)$ is a function of time, changing as the plume moves across the sky. It was observed that the plume moved generally toward the camera as it expanded. If the plume segment that was being viewed moved directly toward the camera, then (see Figure 9a)

$$D(t) = H/\sin(\alpha_0 + \Omega t), \tag{2}$$

where H is the altitude, which was assumed not to change (i.e., the winds have little vertical component) as the plume blew across the sky, α_0 is the elevation before the plume moves (= 55° from Figure 4), and Ω is the angular rate at which the plume moves across the sky.

This is the maximum correction since it is unlikely that the plume moved exactly toward the camera. Because the camera was not configured for measuring changes in elevation and azimuth, the exact correction is not known. The true expansion rate will be between these two limits.

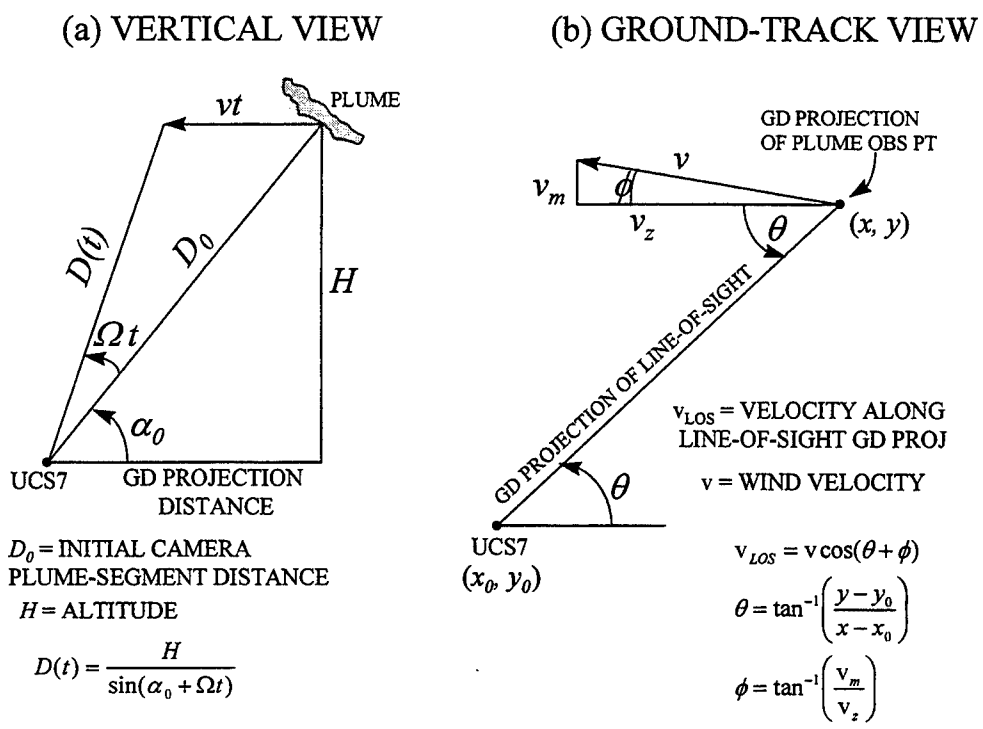

Figure 9. Geometry used to estimate plume motion. (a) View of vertical plane containing plume segment and camera indicating plume motion toward camera position; (b) view of ground track showing meridional and zonal components of the wind. For the initial vehicle position at an altitude of 30 km and the assumed wind direction: x = –80.439°, long., y = 28.711° lat., θ = 27.9°, ϕ = 2.6°.

An estimate of the value of $D(t)$ between the two limits can be obtained from predictions of the stratospheric zonal and meridional winds. These winds are fairly constant for a given season and location and can be used to define the direction of plume motion. In the northern hemisphere during July at an altitude of 30 km, the predicted zonal (E–W) wind velocity is –22 m/s (from the east), and the meridional winds have predicted velocities of about +1 m/s (from the south)[6] based on the NASA/AF Range Reference Atmosphere.[13] Using this predicted wind to define the direction of the motion of the plume (see Figure 9b), we find that a fraction of 0.86 of the plume velocity is projected along the camera line-of-sight. This projection defines the component of the plume velocity that decreases D(t); the orthogonal projection of the velocity increases $D(t)$, offsetting partially this decrease. The plume velocity direction is easily incorporated into the analysis by noting

$$D(t) = \sqrt{(x_0 + v_x t)^2 + (y_0 + v_y t)^2 + H^2}\,, \tag{3}$$

where x_0 = 10.0 km, y_0 = 18.8 km, H = 30.0 km, v_x = –1.139 km/min, v_y = 0.052 km/min.

4.2 Results

The center of the plume moved across the sky at an initial rate of 1.75°/min., a rate that increased by about 10% over a 10-min time period as expected if the plume were approaching the camera at a constant velocity. This angular velocity corresponds to a wind velocity of 19±2 m/s (67 km/hr) at an altitude of 30 km and a range of 36.6 km. Using the wind direction defined by the model discussed above, we find a zonal component of 19 m/s and a meridional component of 1 m/s.

A few seconds after the vehicle passed an altitude of 30 km, a bulge appeared in the plume (see Figures 10 and 11). The time required for the vehicle to pass between the location were the bulge occurred to the narrower diameter marked at T + 90s was about 0.75 s, which corresponds to an altitude difference of 0.5 km. Expansion rates were measured at both the bulge at an altitude of 29.5 km and the plume at an altitude of 30 km to indicate the variability of the expansion rates possible at very closely spaced altitudes.

The diameters as a function of time for the plume and the bulge are shown in Figures 12 and 13, respectively. The values presented are an average of measurements made using the visible and infrared short focal lens instruments (cameras #2 and #4 in Table 2). It was observed that the contrast was better for the infrared camera. Changing the angle of the polarizer during the observation did not markedly change the contrast of either of the visible or infrared images, as expected; however, as noted above, gearing of the polarizer adjustment knob made it difficult to change the polarization angle fast enough to visually perceive a contrast change.

The data at 30 km were acquired for only 12 min, even though the sun did not set at this altitude for another 3 min because the plume width grew to be larger than the FOVs of the cameras. The plume was still visible during this additional 3 min. The width of the bulge was measurable for only 7 min before it expanded beyond the cameras' FOVs. The solid lines and solid circle in these plots display the inferred diameters using a constant value for the distance between the camera site and plume observation point. The open circles and the dotted lines show the effect of applying the maximum correction for decreasing camera-plume separation, as discussed above. The maximum correction lowers the expansion rate by about 15%. As noted above, the true diameters and expansion rates will lie between these two sets of values. Using the predicted wind direction given above to correct for the plume motion yields an expansion rate of 0.50±0.03 km/min at an altitude of 30 km and 0.67±0.05 km/min for the bulge at an altitude of 29.5 km. The uncertainties are those obtained on the slope for a regression fit to an assumed linear function (correlation coefficient values of 0.995 and 0.996 for the plume and bulge fits, respectively). It is interesting to note that the expansion rate of the bulge is also linear and nearly 40% greater than that of the plume even though the bulge is separated by an altitude difference of only 0.5 km.

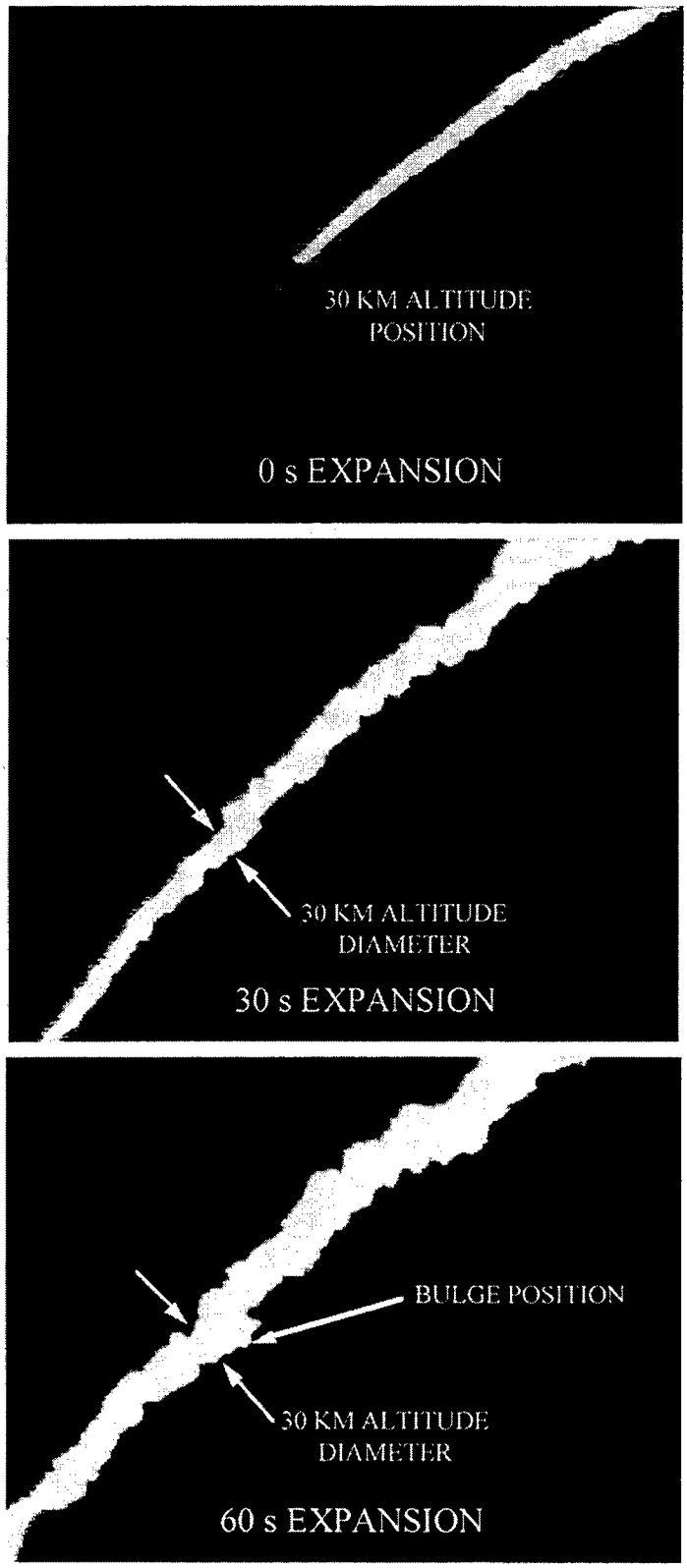

Figure 10. First 60 s of expansion.

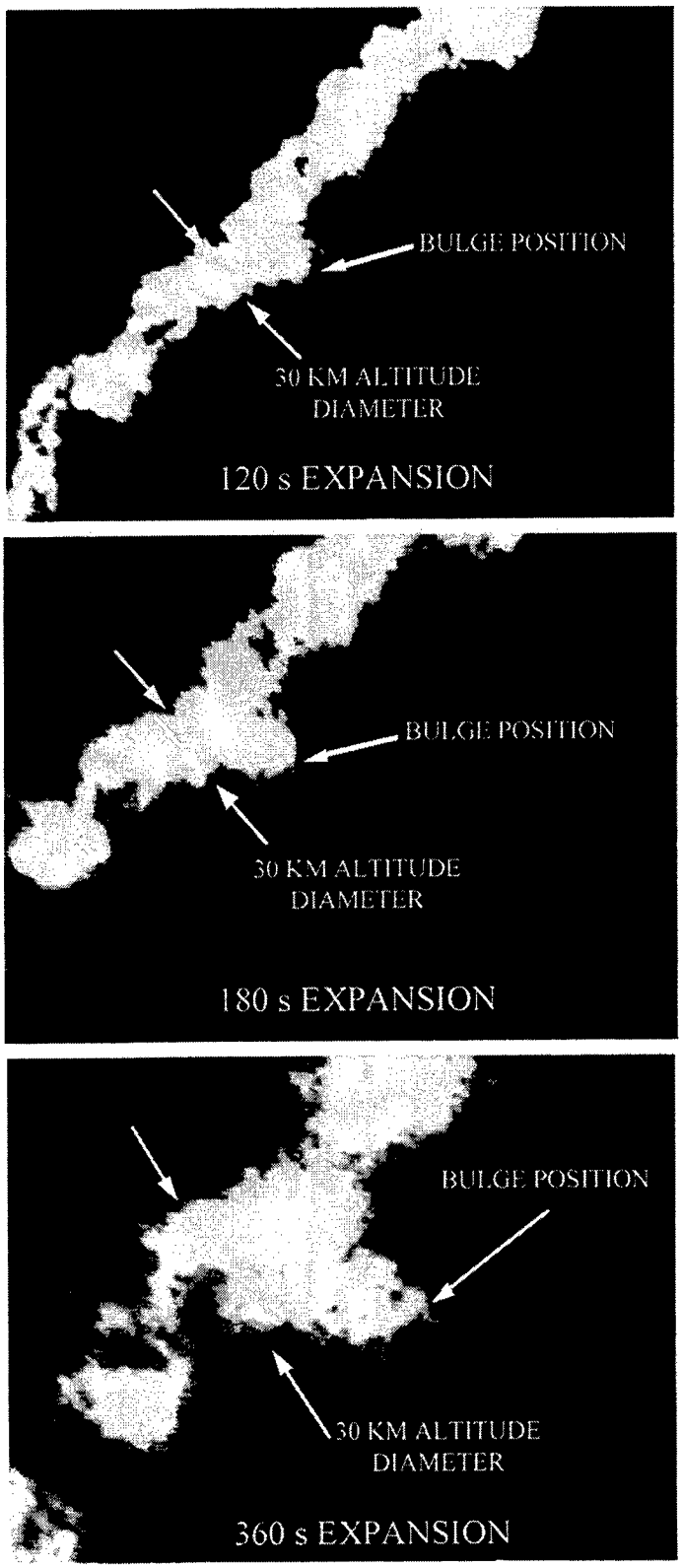

Figure 11. Expansion to 6 min.

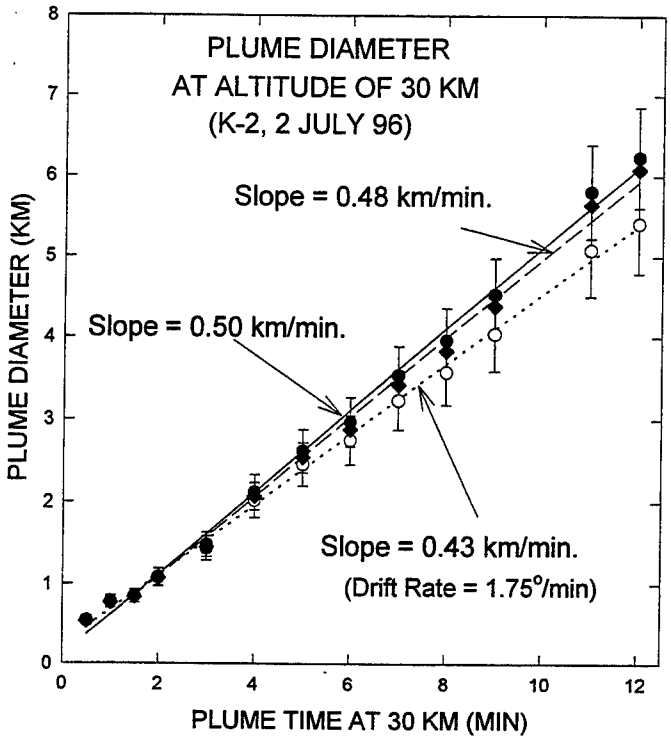

Figure 12. Diameter of the plume at an altitude of 30 km for 12 min after vehicle passage.

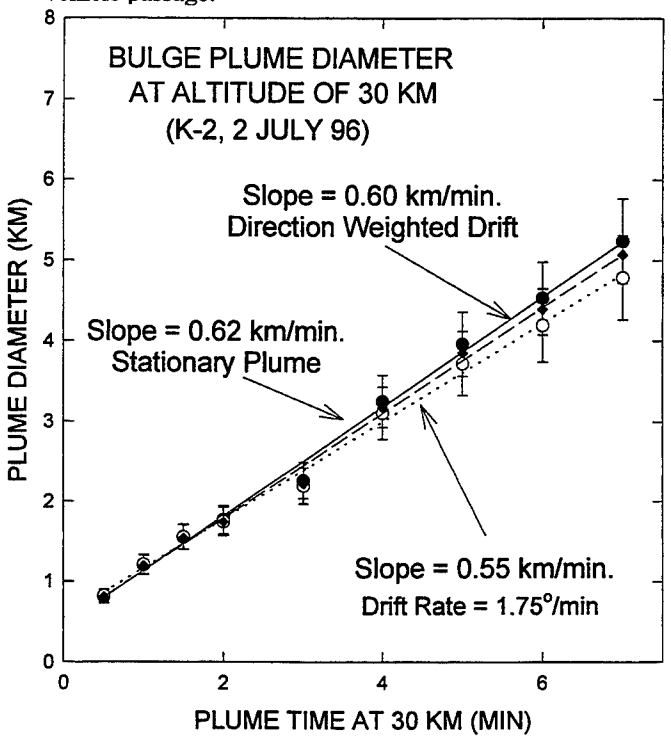

Figure 13. Diameter of the bulge in the plume at an altitude of 29.5 km for 7 min after vehicle passage.

Table 3 compares the expansion rates from previous observations. The value reported by Hoshizaki[8] for a Titan III SRM at an altitude of 18 km is the smallest. The rate reported recently by Beiting[7] for a Titan IV at 30 km is twice the Hoshizaki rate. The rate reported in this report for the plume falls between these two previously reported rates. The rate for the bulge is slightly higher than the previous measurement at the 30 km altitude. The other rates listed in this table are estimates that were indirectly inferred by Beiting[7] from fly-through data taken near 18 km.

Table 3. Expansion Rate Comparison

Measurement	Type	Altitude (km)	Duration (min)	Expansion Rate (km/min)
Hoshizaki [8]	Film	18	10	0.3
Pergament et al. [14]	Fly-through	18	(12)*	(0.3)**
Strand et al.[15]	Fly-through	19	(7,13)*	(0.15-0.5)**
Beiting [7]	Visible Video	30	10	0.6
This Work	IR and Visible Video	30	12	0.48 - 0.60

* Time after SRM passed through the indicated altitude that plane that flew through the plume.

**These values were inferred from pilot estimated times of plume traversal time and aircraft speed.

5. Conclusions

The K-2 launch, which took place 6 min after ground-level sunset, afforded an exceptional opportunity to observe a Titan IV plume expansion under nearly ideal conditions. High-contrast images were recorded throughout the 15-min interval when the plume was illuminated by sunlight because the sunlight scattered from the troposphere was greatly reduced. Had the sun not set at the observational altitude, the morphology of the plume could have been studied for longer times. The results indicate that there is a 40% variability in the expansion rate at adjacent altitudes. Within the uncertainty of the measurements, the expansion rate was constant during the 12-min observation window. The expansion rate of the bulge section of the plume measured here was the same as the expansion rate of the K-10 plume measured at an altitude of 30 km reported previously. It is interesting to note that very little plume drift was observed during the recording of the K-10 plume expansion. The expansion rate of the plume section measured at an altitude of 30 km (which appeared to be more typical of the rates at adjacent altitudes) was 60% greater than the rated previously reported by Hoshizaki at an altitude of 18 km.

The decision to acquire the data presented in this report was made a few weeks before the launch of K-2. The nearly ideal launch conditions, quality of data obtained, and experience gained from the field campaign fully justified the effort. However, because it took advantage of an existing instrument that was not designed for this type of observation, a more suitable instrument is being assembled. Changes from the instrument used here include: azimuth and elevation readouts on the cameras to tract plume motion; wider field-of-view lenses to permit longer viewing times; independent cameras aimed at different altitudes to study the altitude dependence of the expansion rate; polarizers mounted to permit rapid and individual rotation of polarization angles; greater infrared wavelength response to enhance the contrast between the Mie scattered light (signal) from the plume and the Rayleigh scattered light from the troposphere (background); and greater pixel digitization depth for image processing. Future campaigns may use multiple sites to discover the true three-dimensional shape of the plume and aid in the identification of plume breakup

Several outstanding topics can be addressed with these additional campaigns. The first is the altitude dependence of the dispersion. Altitude-differentiated data will allow models of plume chemistry to be developed that will be applicable throughout the stratosphere. Similarly, measurements throughout the year at both the eastern and western test ranges will elucidate any seasonally and geographically dependent plume characteristics. Higher-contrast images will discover the fate of the plume at longer times. Specifically, does the expansion continue at a linear rate and hold together, or does it break up and shear into individual volumes that do not further dilute? The answer to this question also has important consequences for the chemical models used to predict the local ozone depletion. Finally, it would be quite useful if the viewing interval could be extended to the time where the RISO flight and LIDAR data begin. These longer viewing times will permit the overall morphology of the plume to be discovered, providing a context in which those data may be more readily interpreted.

References

1. P. F. Zittel, "Local effects of large, solid rocket motors on stratospheric ozone," The Aerospace Corporation ATR-92(9558)-2; "Computer model predictions of the local effects of large, solid-fuel rocket motors on stratospheric ozone," The Aerospace Corporation TR-94(4231)-9.

2. M. R. Denison, J. J. Lamb, W. D. Bjorndahl, E. Y. Wong, and P. D. Lohn, "Solid rocket exhaust in the stratosphere: Plume diffusion and chemical reactions," AIAA 92-3399, July, 1992: also in *J. Spacecraft & Rockets* **31**, 435–442 (1994).

3. B. C. Kruger, M. M. Hirschberg, and P. Fabian, "Effect of solid-fueled rocket exhausts on the stratospheric ozone layer," *Ber. Bunsenges. Phys. Chem.* **96**, 268–272 (1992).

4. B. C. Kruger, "Ozone depletion in the plume of a solid-fuel rocket," *Ann. Geophysicae* **12**, 409–416 (1995).

5. B. B. Brady and L. R. Martin, "Modeling solid rocket booster exhaust plumes in the stratosphere with SURFACE CHEMKIN," The Aerospace Corporation, TR-95(5231)-9 (1995).

6. M. Ross, "Local Impact of Large Solid Rocket Motor Exhaust on the Stratospheric Ozone," *J. Spacecraft & Rockets*, 33, 144–153 (1996)(1995).

7. E. J. Beiting, "Characteristics of Alumina Particles from Solid Rocket Motor Exhaust in the Stratosphere," The Aerospace Corporation, TR-95(5231)-8; "A Model for Alumina Particles from Solid Rocket Motor Exhaust in the Stratosphere," *J. Spacecraft Rockets*, 1996, submitted.

8. H. Hoshizaki, (Chairman), "Aircraft Wake Microscale Phenomena," Chap 2, pp 60–73, in *The Stratosphere Perturbed by Propulsion Effluents*, edited by G. D. Robinson, H. Hidalgo, and N. Sundararaman (1975). Volume 4 of the CIAP monograph series. U.S. Department of Transportation Rept. No. DOT-TST-75-53. (Available for NTIS as PB249684).

9. R. M. Ehlers, "Validation of Titan IV K-2 TAG Trajectory," The Aerospace Corp. IOC A96-5447.2-015, 17 May 1996 .

10. U.S. Naval Observatory Sunrise-sunset Computation Web Page, http://tycho.usno.navy.mil/srss2.html.

11. R. A. Klingberg and K. C. Herr, "The Spectral Comparative Imager Proof of Concept," ATR-96(8293)-1 (1996).

12. Kinemetrics True Time GOES Satellite Clock, Model 468-FPC, IRIG-B output format.

13. Anon., Range Ref. Atm., "Range Commanders Council," Doc. 361-383, White Sands, NM (1983).

14. H. S. Pergament, R. I. Gomberg, and I. G. Poppoff, "NO_x Deposition in the Stratosphere from the Space Shuttle Rocket Motors," Appendix G to *NASA Tech. Memo. Z-58198*, G-3, Han 1977.

15. L. D. Strand, J. M. Bowyer, G. Varsi, E. G. Laue, and R. Gauldin, "Characteristics of Particles in the Exhaust Plume of Large Solid-propellant Rockets," *J. Spacecraft,* Vol. 18 (4), 1984, pp. 297–305.

THE AEROSPACE CORPORATION
2350 E. El Segundo Boulevard
El Segundo, California 90245-4691
U.S.A.